ASAS-SN Observations of Twelve Quasi-Stellar Objects in the M92 Globular Cluster Field

Abstract The AAVSO International High Energy Network (HEN) is dedicated to the optical monitoring of high energy astrophysical phenomena in the universe. There are multiple high energy objects including Active Galactic Nuclei (AGN), BL Lacertae (BLLAC), Blazars, Gamma Ray Bursts (GRB), and Quasi-Stellar Objects (QSO). A QSO (also known as a quasar) is an extremely luminous AGN, in which a supermassive black hole with a mass ranging from millions to billions times the mass of the sun is surrounded by a gaseous accretion disk. As gas in the accretion disk falls toward the black hole, an enormous amount of electromagnetic energy is released. In spite of this tremendous energy output, the QSO is one of the most difficult objects to observe due to its enormous distance from earth. In order to make accurate QSO observations, telescopes need to spend a great deal of time on target. One of the systems that is capable of making such observations is the All Sky Automated Survey for Supernovae (ASAS-SN) which automatically surveys the entire visible sky every night down to 18th magnitude. This paper presents ASAS-SN observations of twelve QSO located in a field of intermediate galactic latitude centered on the M92 globular cluster.

1. Introduction

The AAVSO International High Energy Network's Target Tool (HET) contains numerous high energy objects that have a widely varying number of observations. Some objects are observed routinely, while others have no observations at all. Among those objects in the HET that have no observations in the AAVSO database are twelve Quasi-Stellar Objects located in the M92 globular cluster, located in the northern constellation of Hercules.

Among the Milky Way population of globular clusters, M92 is among the brighter clusters in terms of absolute magnitude. It is also one of the oldest clusters. M92 is located around 16×10^3 light years (4.9 kiloparsecs or kpc) above the galactic plane and 33×10^3 light years (10 kpc) from the Galactic Center. The heliocentric distance of M92 is 26.7×10^3 light years (8.2 kpc). The half-light radius, or radius containing half of the light emission from the cluster, is 1.09 arcminutes, while the tidal radius is 15.17 arcminutes. It appears only slightly flattened, with the minor axis being about 89% ± 3% as large as the major axis. Characteristic of other globular clusters, M92 has a very low abundance of elements other than hydrogen and helium; what astronomers term its metallicity. Relative to the Sun, the abundance of iron in the cluster equates to only 0.5% of the solar abundance. This puts the estimated age range for the cluster at 11 ± 1.5 billion years.

The twelve QSOs in M92 that have no data in the AAVSO database are: V0396 Her, V0700 Her, V0752 Her, V0754 Her, V0755 Her, V0756 Her, V0758 Her, V0762 Her, V0763 Her, V0764 Her, V0765 Her, and V0766 Her. These objects have been continuously observed by the ASAS-SN

system. ASAS-SN currently consists of 24 telescopes distributed around the globe in both the northern and southern hemispheres.

2. Methods

2.1 Analysis Method

For each of the twelve QSOs in the M92 field, the VSX page has a pulldown menu in the "External Links" section which includes numerous sources of data on the object under study. One of these is the ASAS-SN Sky Patrol which is used to compute light curves of the object. The light curve computation page has preloaded J2000 right ascension and declination information of the QSO being analyzed and a default "number of days to go back" of 20 days (each object is continuously being updated virtually every day). To get a reasonable light curve, 2000 days was used instead of the default 20 days. The computed results yield data in several formats. For this analysis, the CSV (Comma Separated Variable) was selected.

For the selected images, the ASAS-SN photometry is done using the IRAF apphot package and calibrated using the AAVSO Photometric All-Sky Survey (APASS, Henden et al. 2012). The signal is taken from a 2 pixel radius aperture, i.e., about 2 Full Width Half Maximum (FHWM) in diameter and the background is estimated in a 7 to 10-pixel radius annulus. The background pixels are clipped at 2. The aperture photometry is done both for the target position and 100 nearby $11.5 < V < 14$ mag APASS stars with photometric uncertainties less than 0.075 mag. The APASS magnitude range is chosen to avoid saturation and minimize crowding. The APASS stars are also required to have no other APASS star within 56.″25 (about 3 ASAS-SN FWHM) in separation and 5 mag in flux.

The ASAS-SN photometry calibration is set by the median difference between the APASS and instrumental aperture magnitudes for each image after iteratively clipping the APASS calibration stars at a threshold where it would be expected to lose one or fewer stars given Gaussian errors. It is assumed that any dispersion larger than 0.15 mag is dominated by outliers and this is used as a maximum for the estimated dispersion. After clipping the calibration sample, the weighted mean is used as the final calibration. The returned light curve gives the HJD (Heliocentric Julian Date) and UT (Universal Time) dates of the observation, the camera name (e.g., ba, bh, etc.), the FWHM (for monitoring any residual focus issues), the estimated 5-sigma detection limit for the location, the aperture magnitude and its uncertainty, and the flux estimate and its uncertainty (in milli-Janskys or mJy). The aperture magnitude becomes the 5-sigma detection limit once it is below the detection limit. However, the fluxes are always the real flux measurements and their uncertainties and so can be easily combined across images even when the magnitude is only reported as a limit.

For each of the twelve QSO's under investigation, the CSV data was downloaded from the ASAS-SN website. Using the "Star from ASAS-SN File" plugin in the VStar "File" pulldown

menu, the data is loaded into VStar. A “Parameters” window appears with several options for data presentation. The default options are: Load V magnitudes; Load g magnitudes; and Load 5 sigma/excluded observations? Other options are; Load ASAS-SN V magnitudes as Johnson V?, and Load ASAS-SN g magnitudes as Sloan g?. For each QSO, all options were used. The light curve result for each is shown below.

2.2 Analysis Results

The light curves from the twelve QSOs show the ASAS-SN observations for 2000 days prior to XXX yy-zz, 2020. This results in observations for five “observing seasons”, with a brief period of time between seasons without any observations. There is also the beginning of a sixth observing season. This is shown in Figures 1-12.

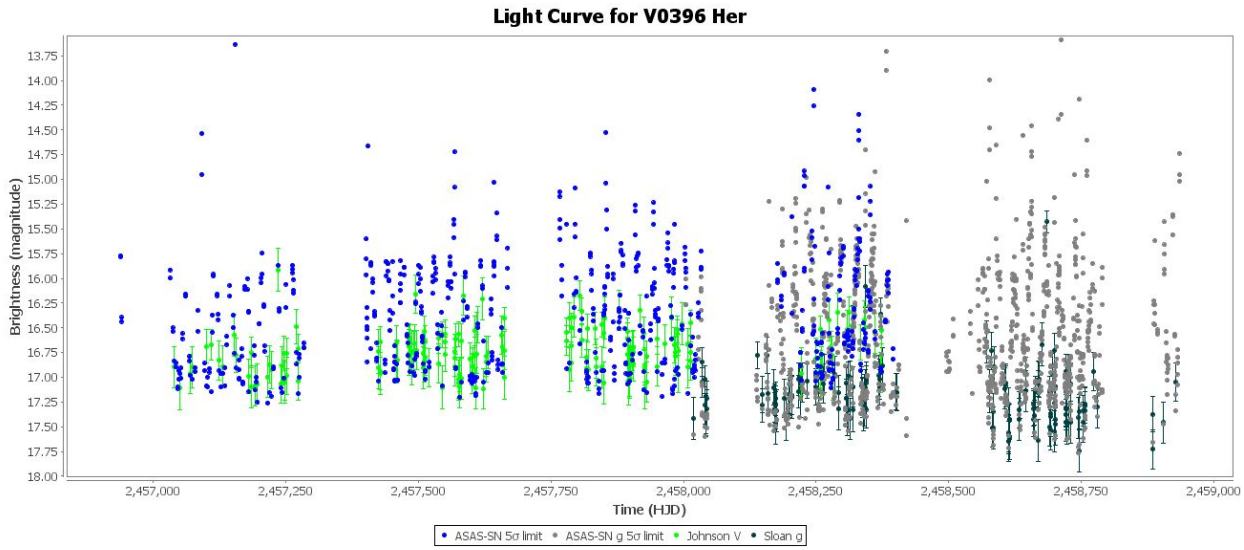

Figure 1: Light Curve for V0396 Her

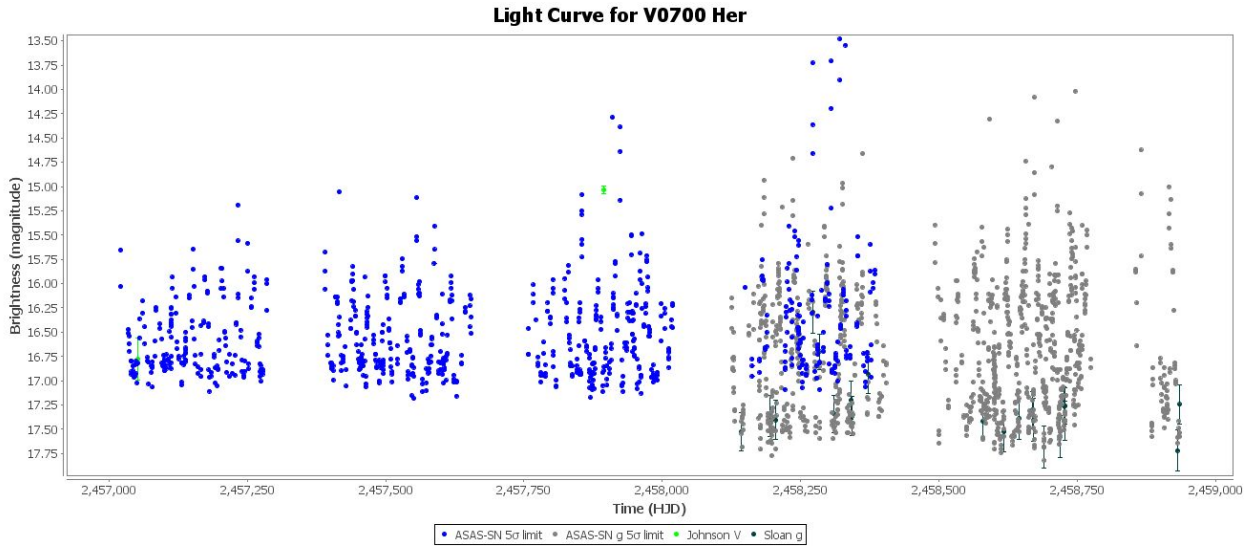

Figure 2: Light Curve for V0700 Her

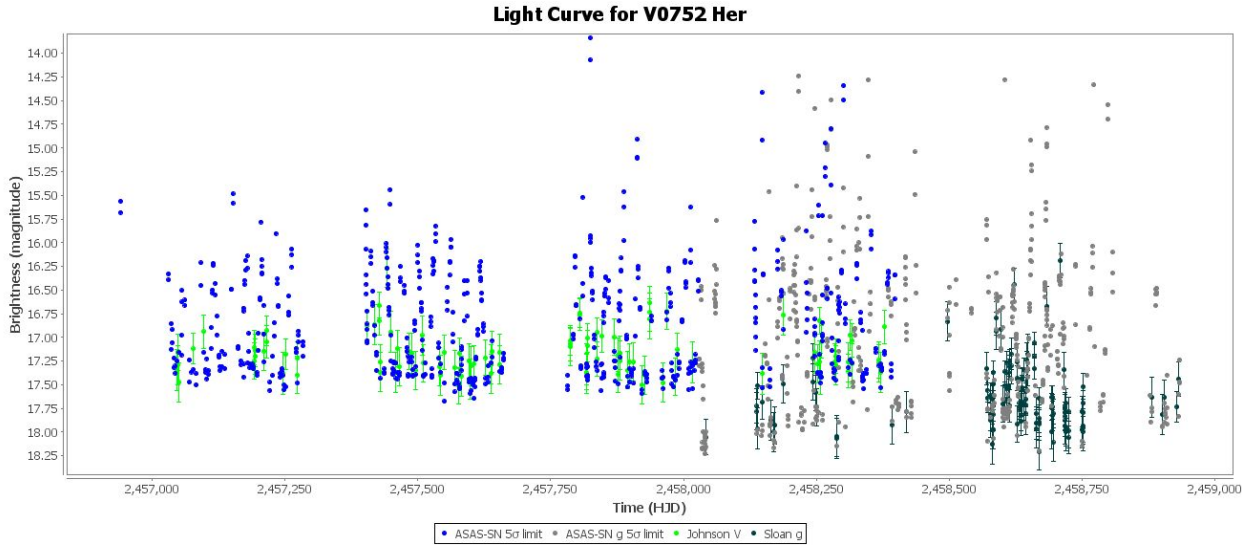

Figure 3: Light Curve for V0752 Her

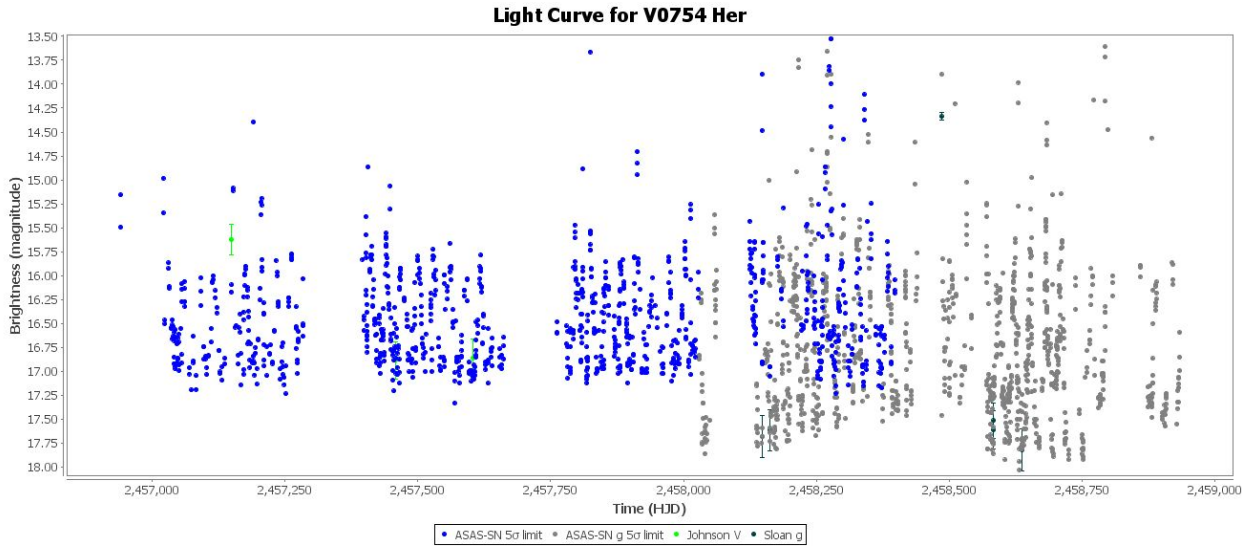

Figure 4: Light Curve for V0754 Her

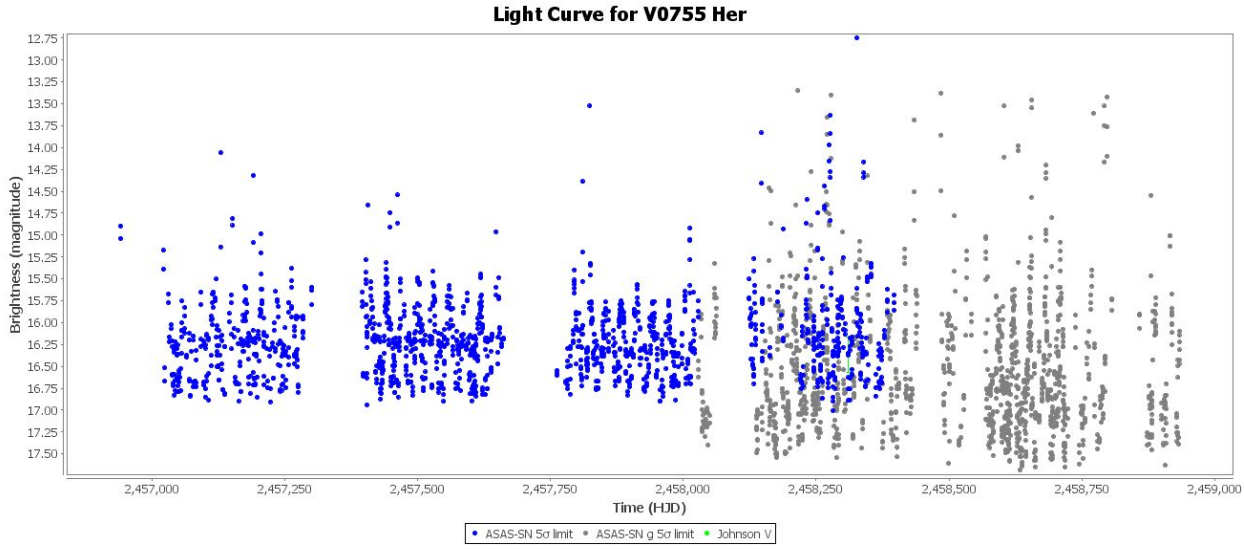

Figure 5: Light Curve for V0755 Her

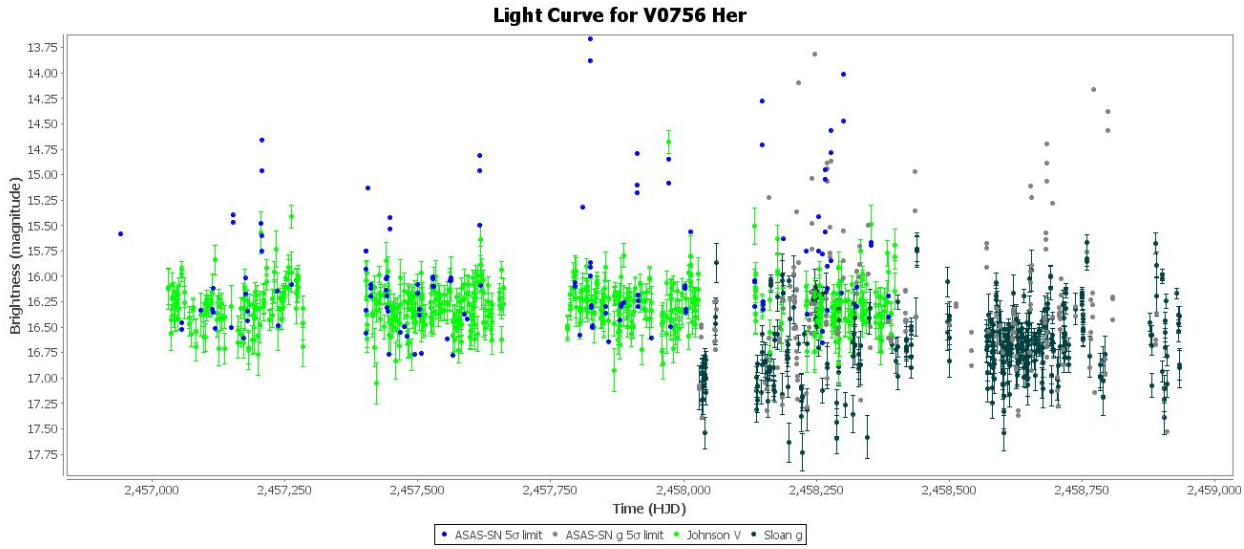

Figure 6: Light Curve for V0756 Her

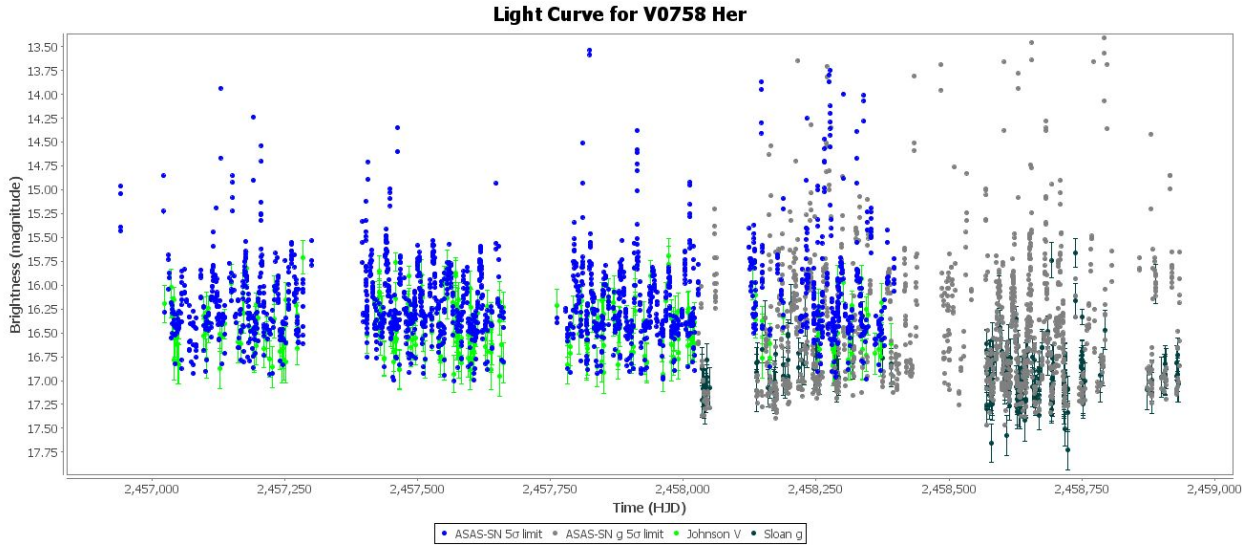

Figure 7: Light Curve for V0758 Her

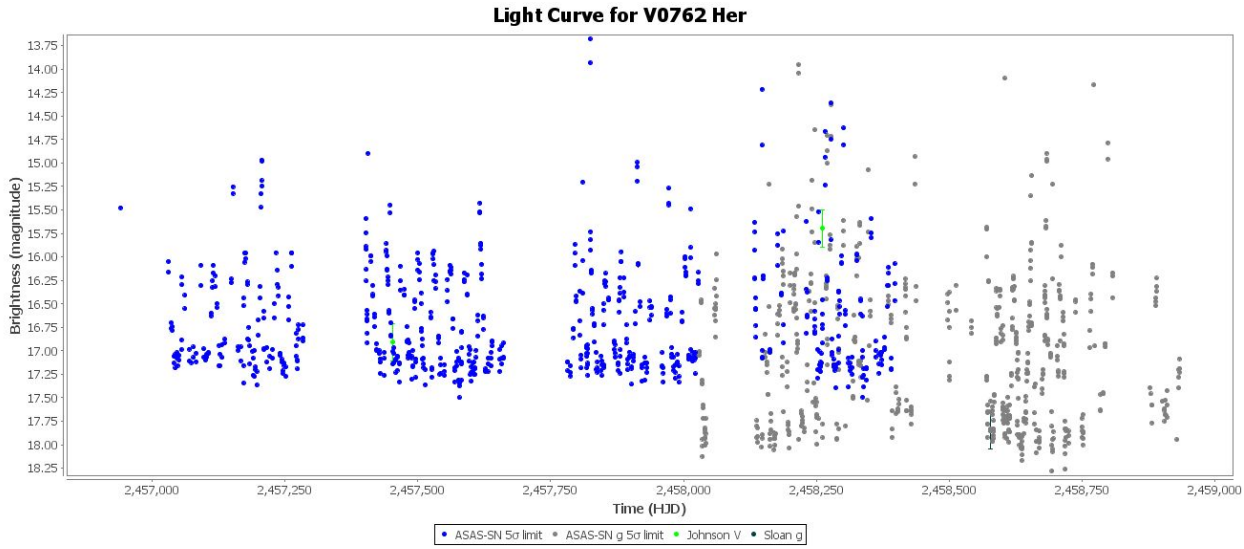

Figure 8: Light Curve for V0762 Her

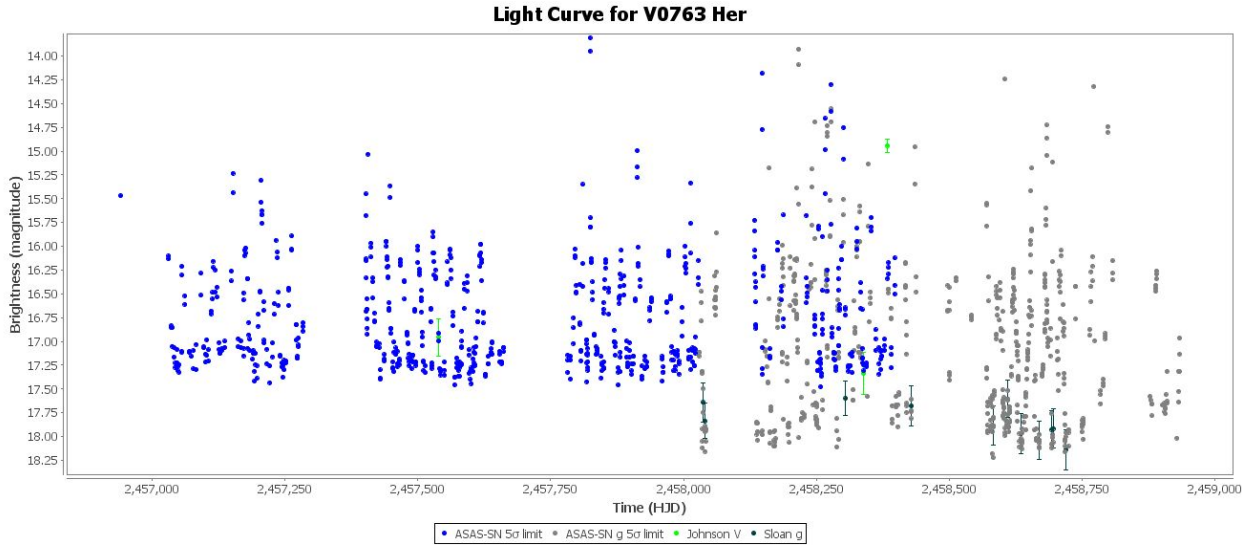

Figure 9: Light Curve for V0763 Her

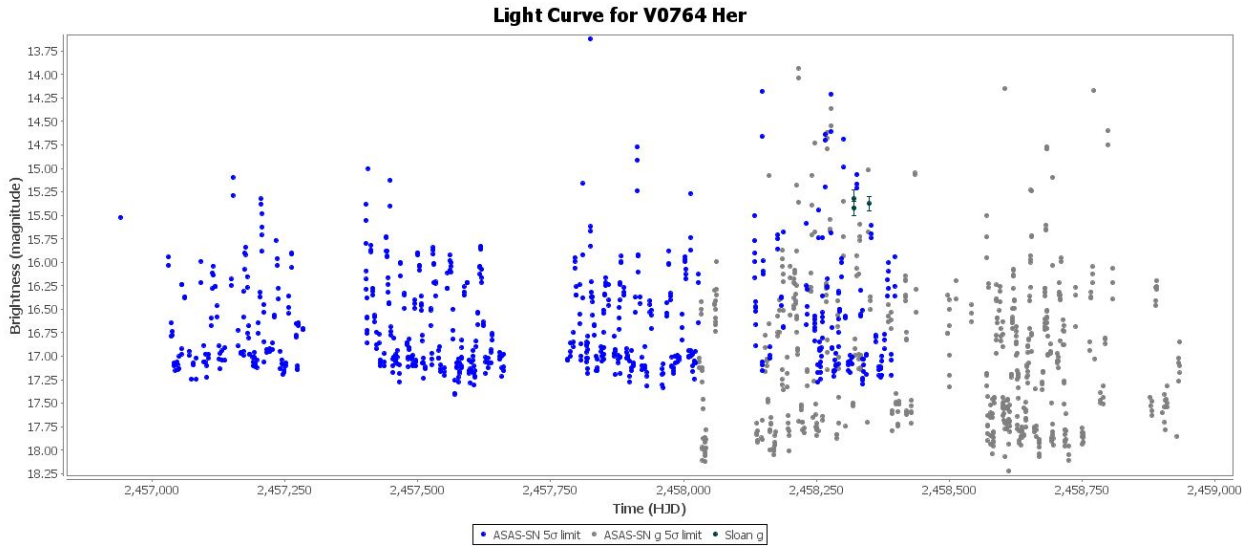

Figure 10: Light Curve for V0764 Her

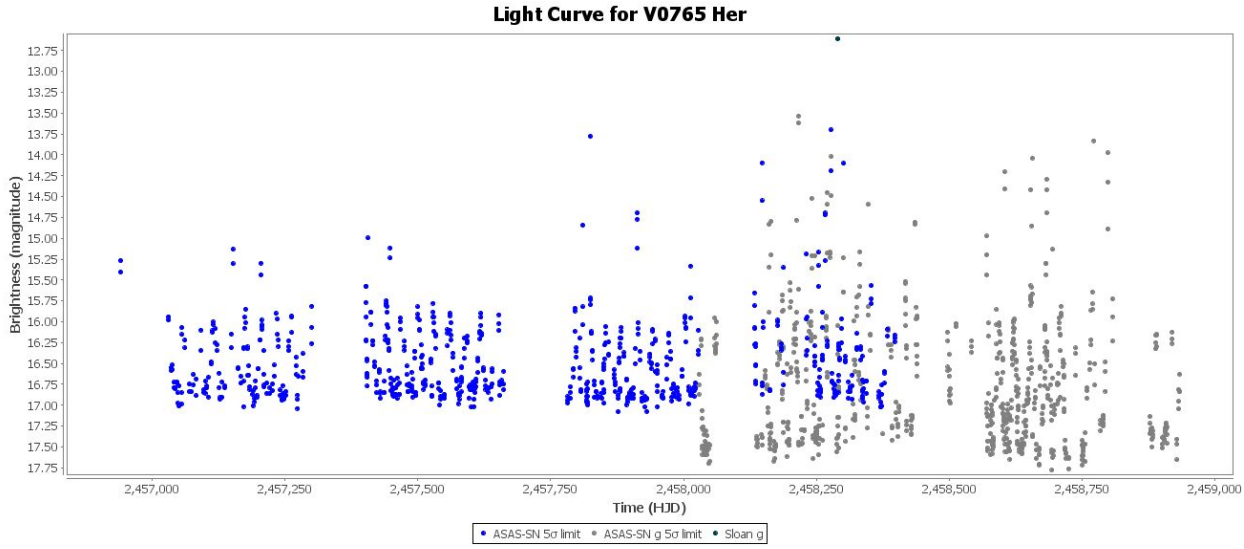

Figure 11: Light Curve for V0765 Her

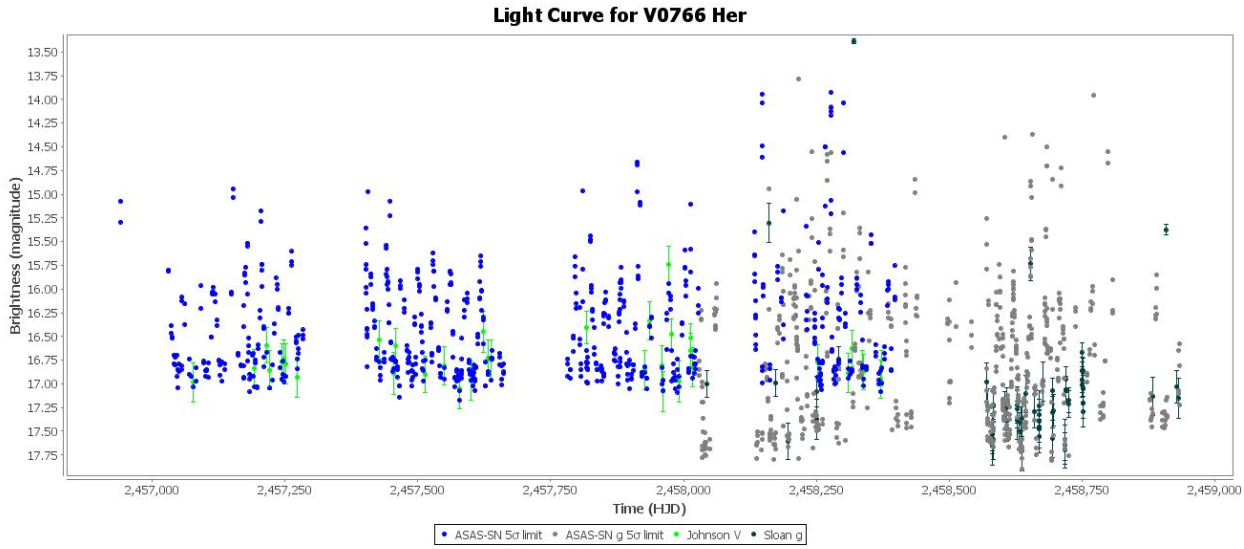

Figure 12: Light Curve for V0766 Her

For the purpose of analyzing a typical QSO, V0756 Her was chosen as an example for performing a more detailed investigation. Specifically, the power spectrum (DC DFT period analysis) is shown for each of the observation bands, i.e., Johnson V, Sloan g, ASAS-SN 5 sigma limit, and ASAS-SN g 5 sigma limit. These are shown in Figures 13 through 16, respectively.

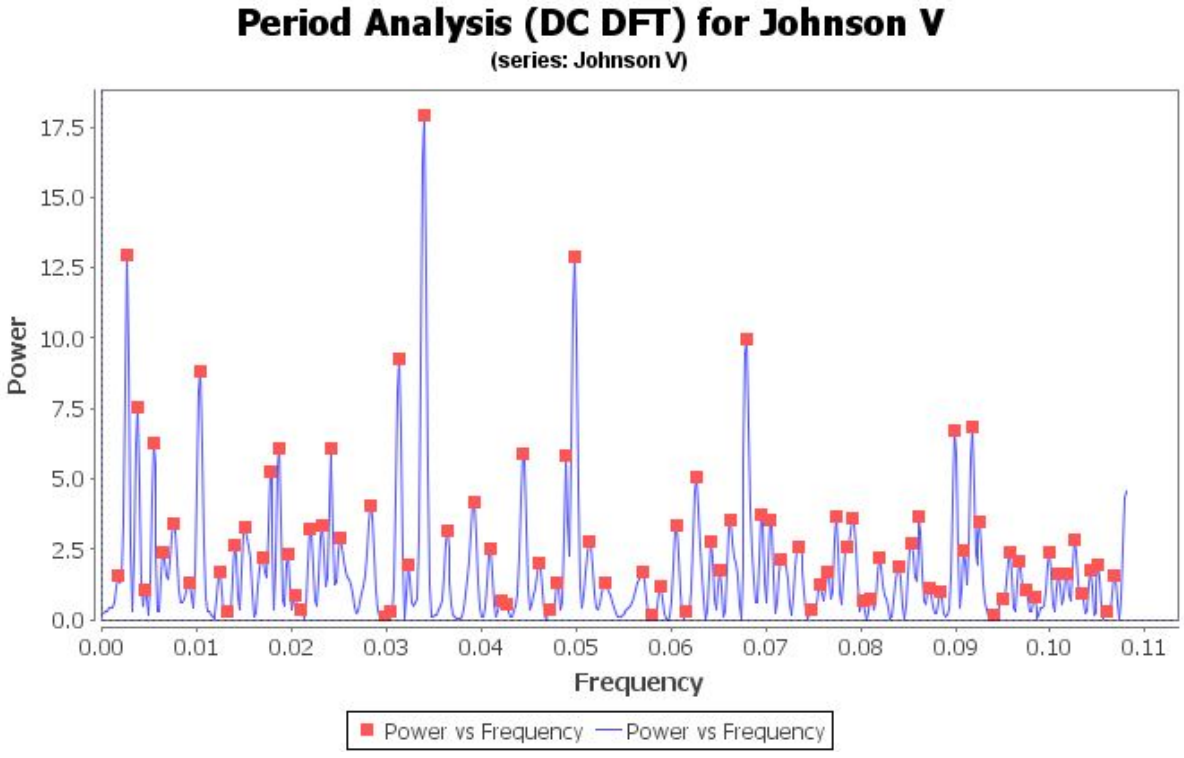

Figure 13: Power Spectrum for Johnson V

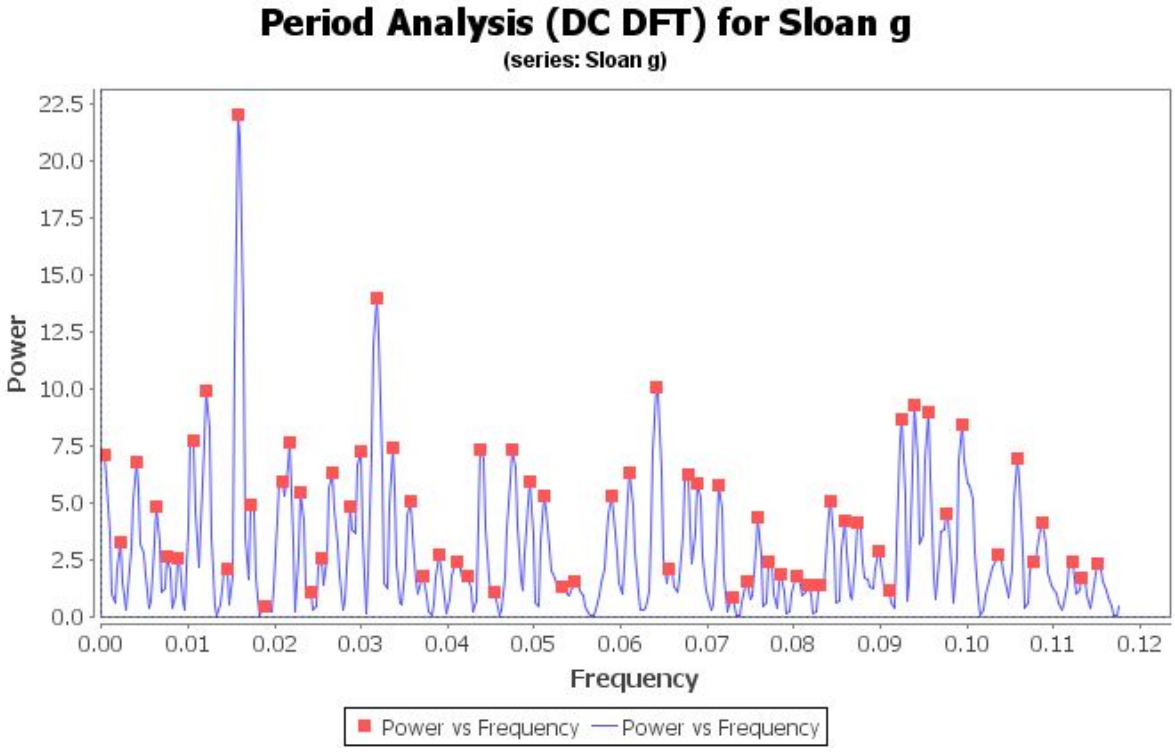

Figure 14: Power Spectrum for Sloan g

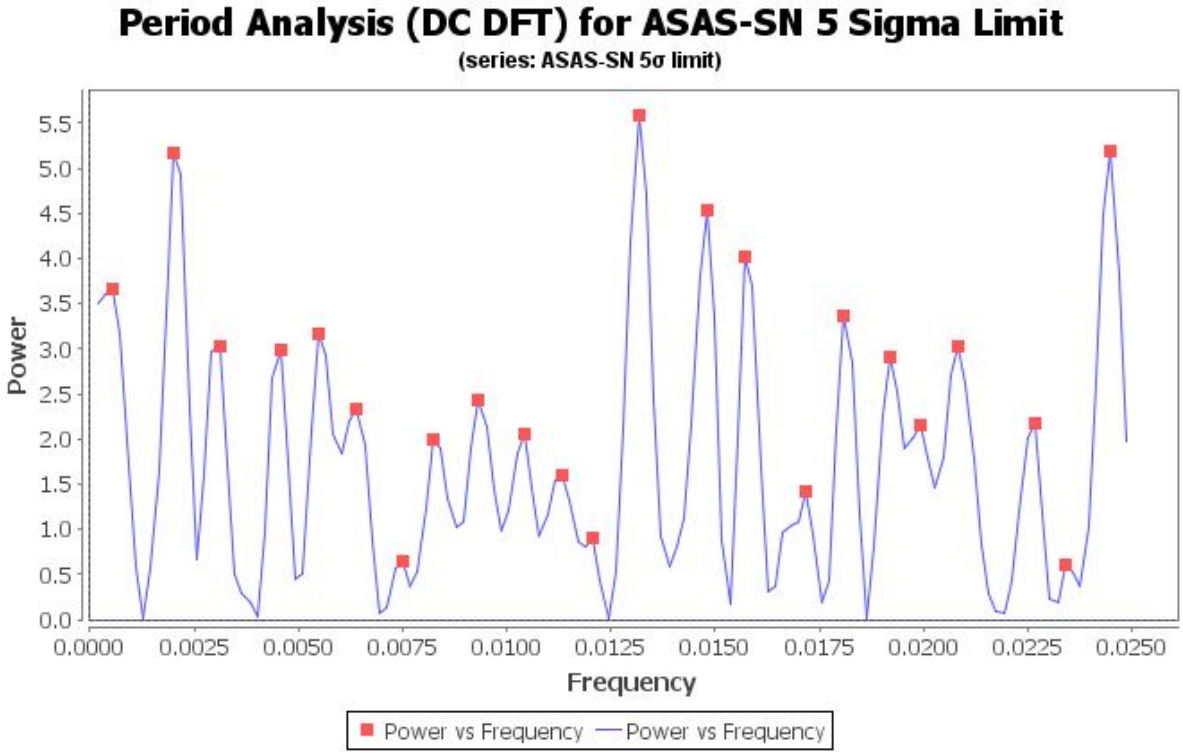

Figure 15: Power Spectrum for ASAS-SN 5 Sigma Limit

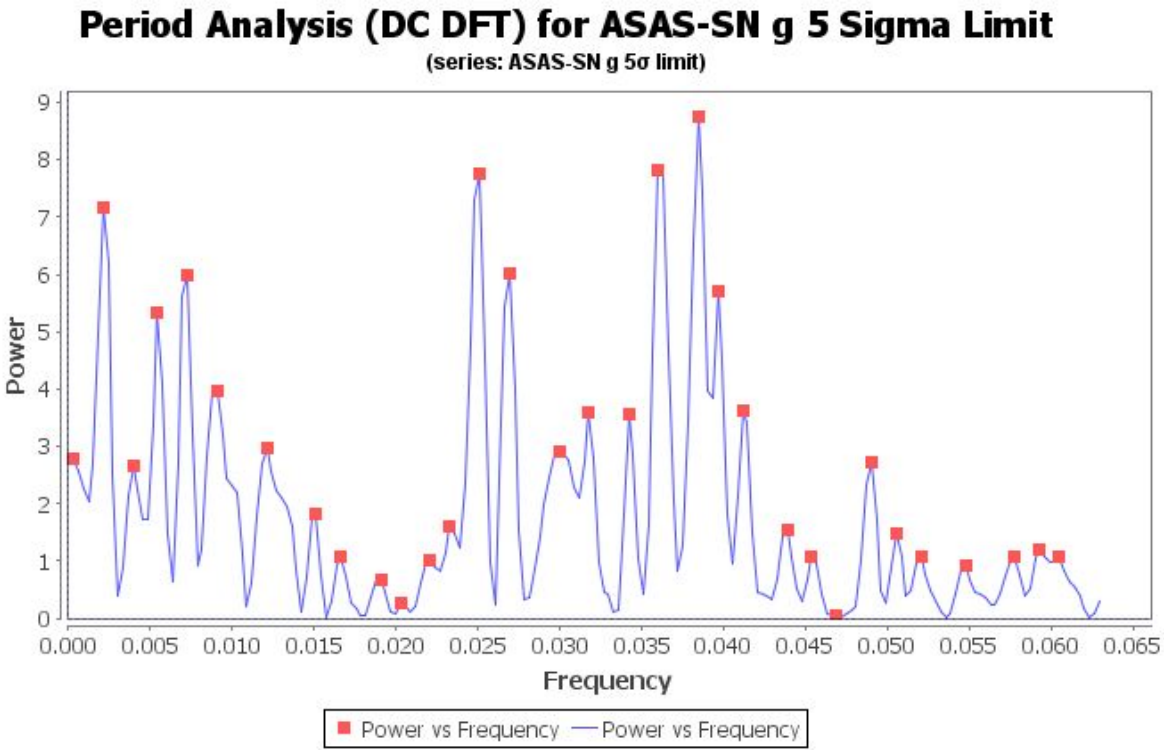

Figure 16: Power Spectrum for ASAS-SN g 5 Sigma Limit

2.3 Discussion

As can be seen for each of the four ASAS-SN observational bands, there is a great deal of variability in the power with respect to frequency as well as the specific observational bands. QSO luminosities are variable, with time scales that range from hours to days to months to years. Variability is likely due to accretion disk instabilities. The QSO is an extremely luminous AGN, in which a supermassive black hole with a mass ranging from millions to billions times the mass of the sun is surrounded by a gaseous accretion disk. As gas in the accretion disk falls toward the black hole, an enormous amount of electromagnetic energy is released across the entire observable spectrum from radio waves, infrared, visible light, ultraviolet, X-rays, and gamma rays.

Light and other radiation cannot escape from within the event horizon of a black hole. The energy produced by a QSO is generated outside the black hole, by gravitational potential energy stresses and immense friction within the material nearest to the black hole, as it orbits and falls inward. The huge luminosity of QSOs results from the accretion discs of central supermassive black holes, which can convert between 6% and 32% of the mass of an object into energy, compared to just 0.7% for the proton-proton chain nuclear fusion process that dominates the energy production in Sun-like stars. The matter accreting onto the black hole is unlikely to fall directly in, but will have some angular momentum around the black hole that will cause the matter to collect into the

accretion disk. QSOs may also be ignited or re-ignited when normal galaxies merge and the black hole is infused with a fresh source of matter.

Additionally, optical variability is correlated with other properties such as rest-frame wavelength, redshift due to the metric expansion of space, absolute magnitude and luminosity, variability on multiple timescales (e.g., thermal timescales), observational time-lag, radio properties, emission line properties, and the existence of relativistic jets produced within the QSO structure. There is also evidence that variability amplitude is related to the mass of the black hole itself since that mass difference may result in variation in the accretion rate. Finally, variability can result from the orientation of the accretion disk and jets relative to the observer and by the degree of obscuration by the gas and dust within the host galaxy.

The variation in flux density over time is one of the key characteristics of active galactic nuclei. For quasars, which are the most luminous active galactic nuclei, variability is known to be a diagnostic property but the physical mechanisms behind these fluctuations are still poorly understood. However, it has long been known that the observed flux variations are important to understanding the structure of the radiation source. The most frequently discussed models for the continuum variability of AGNs include instabilities in the accretion disk, with variability almost always stronger in the bluer passband than in the redder passband. Also, quasars with unusual spectra and weak emission lines tend to have less variability than conventional quasars.

There are several physical time scales that have been identified in a variety of studies. It is possible that the variability seen is not the direct product of a single intrinsic process but a convolution of several. These include:

- viscous (“radial drift”) time scale (on the order of 10,000 yrs)
- dynamical time scale (days to years)
- thermal time scale (days to years)
- light travel time scale (hours to days)

For the light time scale, the large distances and extreme brightness of QSOs imply tremendous energy output. As previously mentioned, QSO luminosities are variable with time scales that range from hours to years. Additionally, QSOs vary in brightness often by a huge amount in very short time periods. This means that QSOs generate and emit their energy from a very small region since each part of the QSO would have to be in contact with other parts on such a time scale as to allow the coordination of the luminosity variations. This implies that the size of a variable, luminous object cannot be larger than the distance that light travels during its time of variation. The variability timescale of a QSO limits the size of its light emitting region. If an object varies significantly in brightness over a period of a week, it cannot be larger than a light-week in size. For

a QSO varying in brightness, light would begin travelling from the center of the QSO and the points along its diameter all at the same time. Light from the center of the QSO would always be a week behind light emitted from the front and reach an observer a week after detection of light from the front. Light from the back would be detected another week later. The variation of the QSO would be observed as a rise and fall in brightness over a two week period. Finally, radiation from QSOs is partially 'nonthermal' (i.e., not due to black body radiation), and approximately 10 percent are observed to also have jets and lobes like those of radio galaxies that also carry significant amounts of energy in the form of particles moving at relativistic speeds.

In the optical, it is only the variability amplitude and its correlation with time scale that have so far been suggested to be related to intrinsic physical parameters. For example, the amplitude of quasar optical variability increases with time lag and decreasing luminosity, decreases with rest-frame wavelength, and Eddington ratio (the limit where gravitational and radiation pressure are balanced; important because it is a measurement of the ratio of energy output of a source to the physical limit of energy output). The structure function tends to possess a steeper slope for quasars with a larger black hole mass. The structure function is a statistical measure of quasar variability based on the time-lag between two observations. The structure function is closely related to the autocorrelation function and contains, as a sort of running variance (as a function of the time-lag), information about the timescales of the involved variability processes. It was first introduced to quasar research in radio astronomy and has also become a popular tool in optical studies of both quasar samples and individual quasar lightcurves. For the dependence of variability on time-lag, the best model is a power-law fit of the sample-averaged structure function.

The sample-averaged variability measured in a given photometric passband is expected to change with redshift because of the dependence of variability on absolute magnitude and intrinsic wavelength. In addition, there might be an explicit dependence of variability on redshift. In an observed light curve, the intrinsic rest frame variation timescale is multiplied by (1+z), which is the redshift, so may be a correlation between the observed variation timescale and redshift.

Models for quasar variability suggest different variation characteristics in different energy bands. The disk instability model predicts that bluer color on a short timescale variability changes to redder color on longer timescales and the negative variability asymmetry on longer timescales should be smaller in higher energy bands. An anticorrelation with variability is plausible because, if the accretion rate is high, the region emitting the continuum observed in a given passband is larger and the variability amplitudes are consequently smaller than in the case of a low accretion rate. Finally, quasars with unusual spectra and weak emission lines tend to have less variability than conventional quasars. This trend is the opposite of that expected from the dilution effect of variability due to line emission and may be indicative of high Eddington ratios in these unusual quasars.

Other physical mechanisms underlying the optical variability have been proposed: the superposition of supernovae, microlensing, thermal fluctuations from magnetic field turbulence, as well as instabilities in the accretion disk. The correlation with black hole mass is still unclear, with different studies advocating either positive or negative relationships, depending on the degree to which observational biases have been eliminated. A relation between black hole mass and quasar metallicity has been suggested.

The relationship between disk size and metallicity may result in large changes in disk opacity as a function of the gas metallicity, which can significantly alter the thermal properties and structure of the accretion disk. This might then explain the connection between variability and luminosity. Alternatively, a large mass accretion rate can also be responsible for a large amount of photon emission from the disk and also a large surface density. The gas pressure at the radius exhibiting a fixed temperature should thus be relatively larger for luminous quasars, and luminous quasars should have accretion disks with a relatively larger scale height (i.e., disk thickness or disk aspect ratio).

The characteristics of the variability asymmetry are in agreement with those from the self-organized disk instability model, which predicts that the magnitude of the variability asymmetry is controlled by the ratio of the diffusion mass to the inflow mass with the asymmetry diminishing as the ratio increases. It has been found that the asymmetry decreases as the luminosity increases which requires efficient mass diffusion in the accretion disks of luminous quasars. This can be interpreted by observational results that quasars with higher metallicity have smaller disk sizes at a fixed wavelength. If it is assumed that the height of the disk is determined by the mass accretion rate at a radius and that the dispersion of the mass accretion rate is small among quasars, then luminous quasars should have a relatively smaller disk and larger scale height at a portion of the accretion disk with fixed disk temperature. Alternatively, the high accretion mass rate could be responsible for a higher accretion disk scale height in luminous quasars. As the scale height is proportional to the diffusion mass rate, luminous quasars should have lower variability asymmetry with lower variability amplitude as the efficient mass diffusion results in fewer large avalanches. This is consistent with previous results in the literature that luminous quasars exhibit lower amplitude variability.

Finally, in looking at Figures 13 through 16, there is likely another source of variability. This is due to the use of the DC-DFT mathematical analysis itself. One problem using Fourier analysis to detect periods is that discrete methods for analyzing unevenly sampled data will produce spectral artifacts of the sampling of the data, in addition to any signal contained within the data. Data taken over a series of nights will have aliases caused by the sampling windows. These alias frequencies are centered on any real signals in the data, offset from the central frequency by integer multiples of sampling rate. The reason for this is that the data sampling produces a window function in the

Fourier transform, which is convolved with the Fourier peak of the "real" signal. The result is an array of frequencies in the Fourier spectrum.

In certain circumstances, it is possible to detect frequencies higher than the sampling rate. The transform will again suffer from aliasing, in which several different peaks appear in the transform, along with the real one. As before, the alias peaks are separated from the true frequency by integer multiples of the sampling frequency, such that the transform will look like a "picket fence" when plotted. In the case of regular sampling, the alias peaks will have equal statistical significance to the real peak, and it is therefore impossible to tell which peak in the power spectrum is the correct one. In the case of uneven sampling, there is still aliasing, but the strengths of the alias peaks will generally be lower than that of the dominant one. In general, one deals with aliasing in the spectrum by assuming the strongest peak observed is the correct frequency.

3. Conclusions

There are several conclusions that can be drawn from this study of twelve Quasi-Stellar Objects in the M92 Globular Cluster. These are:

1. All twelve objects were continuously observed by the ASAS-SN network of ground-based telescopes, resulting in accurate, long term light curve data for each object.
2. The study of the properties of the optical variability of quasars is complicated by the combined effects of the dependence of variability on timescale, observational time-lag, rest-frame wavelength, redshift, radio properties, emission line properties, luminosity, and the presence and structure of jets. It is possible that the variability seen is not the direct product of a single intrinsic process but a convolution of several.

3. In spite of a significant amount of observational data as well as numerous theoretical analyses of QSOs, these objects are still not well understood, although accretion disk instability seems to be the leading candidate for a plausible explanation, with optical variability possibly triggered by variations in the accretion rate.

Acknowledgements

The author would like to thank the AAVSO for the VStar data analysis software without which this work would not be possible.

This paper made use of ASAS-SN photometric data. The author thanks the ASAS-SN project team for their remarkable contribution to stellar astronomy, and for making the data freely available on-line.

This paper also made use of the AAVSO Target Tool/HET Target List to provide the list of the twelve objects as well as detailed technical information about each. The author thanks

Filtergraph in partnership with Vanderbilt University for developing this tool and hosting it on the AAVSO website.

References

Benn, D. 2013, VStar data analysis software (http://www.aavso.org/vstar-overview)

ASAS-SN (https://asas-sn.osu.edu/), Shappee et. al (2014) and Kochanek et. al (2017)

Filtergraph in partnership with Vanderbilt University

Wikipedia. 2020, Messier 92 (https://en.wikipedia.org/wiki/Messier_92)

Wikipedia. 2002 Quasars (https://en.wikipedia.org/wiki/Quasar)

Brunzendorf, J. and Meusinger, H. 2002, "A QSO survey via optical variability and zero proper motion in the M92 field IV. More QSOs due to improved photometry." http://arxiv.org/abs/astro-ph/0206231v1

Brunzendorf, J. and Meusinger, H. 2001, "A QSO survey via optical variability and zero proper motion in the M92 field II. Follow-up spectroscopy and of the QSO sample." A&A 374, 878-894 https://www.aanda.org/articles/aa/pdf/2001/30/aah2793.pdf

Meusinger, H. et al 2011, "Spectral variability of quasars from multi-epoch photometric data in the Sloan Digital Sky Survey Stripe 82" https://www.aanda.org/articles/aa/pdf/2011/01/aa15520-10.pdf

MacLeod, et al 2012, "A Description of Quasar Variability Measured Using Repeated SDSS and POSS Imaging" https://arxiv.org/abs/1112.0679

MacLeod, C. 2017, "A Review of AGN Variability Studies Using Survey Data: Prospects for LSST" https://agn.science.lsst.org/sites/default/files/LSST_AGN_SC_2017_MacLeod.pdf